Available online at www.sciencedirect.com
ScienceDirect
Optics Communications 281 (2008) 1037–1046
OPTICS COMMUNICATIONS
www.elsevier.com/locate/optcom

Optical pulse shaping at moderate power using a twisted-fibre NOLM with single output polarisation selection

O. Pottiez [a,*], B. Ibarra-Escamilla [b], E.A. Kuzin [b]

[a] Centro de Investigaciones en Óptica, León, Gto 37150, Mexico
[b] Instituto Nacional de Astrofísica, Óptica y Electrónica (INAOE), L.E. Erro 1, Tonantzintla, 72000 Puebla, Pue., Mexico

Received 9 May 2007; accepted 7 October 2007

Abstract

We demonstrate theoretically and experimentally that efficient signal shaping operation can be obtained at moderate power by using the transmission characteristic of a power-symmetric nonlinear optical loop mirror (NOLM) including highly twisted fibre and operating through nonlinear polarisation rotation, when the circular polarisation state orthogonal to the input polarisation is selected at the NOLM output. By adjusting the angle of the quarter-wave retarder inserted in the loop, the phase bias of the transfer characteristic can be adjusted precisely to enable proper signal shaping for moderate values of input power, remaining well below switching power. The tolerance of the procedure to deviations of the input polarisation from the ideal circular case is investigated numerically. We demonstrate experimentally the capabilities of this setup for both power equalisation and extinction ratio enhancement. Finally, we show that this setup is also useful to shape ultrashort optical pulses from the relaxation oscillations of a DFB semiconductor laser. In comparison with other NOLM-based techniques, the proposed approach allows to reduce by a factor of 8–10 the peak power required for pulse shaping, for the same fibre length and Kerr coefficient.

PACS: 42.81.−i; 42.79.Ta; 42.79.Sz; 42.30.Lr

Keywords: Sagnac interferometer; Fibre-optic devices; Optical signal processing

1. Introduction

The nonlinear fibre Sagnac interferometer, or Nonlinear Optical Loop Mirror (NOLM) [1] is a versatile device that has been used for various applications, including ultrafast switching, signal processing [2–8] or optical data monitoring [9]. The device exhibits a nonlinear power transmission characteristic, which is a sinusoidal function of input power. Through the adjustment of the phase bias of this function, this transmission characteristic can be adapted to each particular application [2,10]. This phase bias can be adjusted through a tuneable birefringence element inserted in the NOLM, which in most cases takes the form of a polarisation controller (PC). In conventional NOLMs, birefringence is already present in the loop as a result of the residual anisotropy of standard fibre. The PC-induced birefringence thus adds to this uncontrolled birefringence, and the PC is adjusted empirically until the desired transmission characteristic is obtained. Although this blind adjustment procedure allows selecting easily one of the two main modes of operation of the device (saturable absorber or intensity limiter), it is not so convenient when a more precise definition of the phase bias is expected. Moreover, the fibre residual birefringence is very sensitive to environmental perturbations, which causes bias drifts and imposes frequent PC readjustments. Another important issue is that, for most applications, the input power into the NOLM has to be increased up to the switching power, or beyond

* Corresponding author. Tel.: +52 477 4414200x288; fax: +52 477 4414209.
E-mail address: pottiez@cio.mx (O. Pottiez).

0030-4018/$ - see front matter © 2007 Elsevier B.V. All rights reserved.
doi:10.1016/j.optcom.2007.10.080

(i.e. the nonlinear phase difference should reach π or more) [11–13]. This usually makes the device impractical for many applications, as very long pieces of fibre must be used to avoid excessive switching power (still ~15 W for a NOLM made of 1 km of standard fibre and a 0.6/0.4 coupler). Moreover, high powers and long fibre lengths are usually associated with the onset of parasitic nonlinear effects, like stimulated Brillouin or Raman scattering, which limit the device performances.

It was demonstrated recently that standard fibre, when submitted to high twist, behaves like an ideal isotropic fibre [14]. The use of highly twisted standard fibre in a NOLM is thus likely to reduce the problems related to residual birefringence. The behaviour of a NOLM including twisted fibre was first studied in [15], and a scheme including highly twisted fibre was proposed in [16]. For high twist, the isotropic property of the twisted fibre loop prevents nonlinear polarisation rotation (NPR) from averaging out as the beams propagate, allowing NPR to be the main mechanism of switching. Self-Phase Modulation (SPM) is thus not needed, so that a 50/50 coupler can be used, yielding a power-symmetric NOLM design. High twist also improves noticeably the environmental stability of the NOLM. An attractive scheme is obtained by inserting in the highly twisted NOLM a quarter-wave retarder (QW) as the symmetry-breaking element [16]. Among the interesting features of this device appears a high dynamic range, as minimal transmission is virtually zero [17]. We showed previously that this scheme offers great flexibility for the adjustment of the transmission characteristic. In particular, considering a circular input polarisation state, phase bias is readily adjusted through rotation of the QW [18]. Although this procedure offers a simple and well defined way to adjust precisely the phase bias, it also degrades dramatically the dynamic range as the minimum of nonlinear transmission is shifted from zero input power. This device was demonstrated in the frame of amplitude equalisation of an optical pulse train, but a quite high input power exceeding the switching power had to be reached for this purpose [13].

In this Paper, we present a detailed analysis of the power-symmetric NOLM under circular and quasi-circular input polarisation when the orthogonal circular polarisation component is selected at its output. In the frame of signal shaping applications, we demonstrate that the NOLM transmission exhibits attractive features at moderate power, so that it is not necessary to increase the input power up to the switching power for proper signal shaping operation. We demonstrate experimentally the potential of the device for two distinct signal shaping applications: amplitude equalisation and extinction enhancement. We also show how this setup can be used to shape ultrashort optical pulses out of the relaxation oscillations of a DFB semiconductor laser.

2. Theoretical analysis

The scheme that we consider in this analysis is shown in Fig. 1. It consists of a power-symmetric NOLM made of a symmetric coupler, a piece of highly twisted low-birefringence fibre, and a QW (QW_N) inserted in the loop after one of the coupler output arms. We consider that polarisation is circular (say, right) at the NOLM input. A QW (QW_{out}) and a polarizer P are inserted at the NOLM output, with a relative orientation of 45° in the adequate direction so as to select the orthogonal circular polarisation component (say left). We showed previously [19] that, in the weak nonlinearity limit [16], and for high twist (ideal isotropic fibre), the power transmission of the NOLM alone (without QW_{out} and P) is given by

$$T_N = \frac{1}{2} - \frac{1}{2}\cos 2(\alpha - \alpha_c)\cos\left[\pi\frac{P_{in}}{P_\pi} + 2(\alpha - \alpha_c)\right], \qquad (1)$$

where P_{in} is the input power, α is the QW_N orientation and $P_\pi = 4\pi/\gamma L$ is the minimal switching power that can exhibit a power-balanced NPR-based NOLM with fibre length L and nonlinear coefficient γ (in rad/W/km). Zero transmission at low power is ensured by setting the QW_N angle at the critical value $\alpha_c = \beta/2 + k\pi/2$, where k is an integer, and $\beta = \rho L$ (where ρ is the rotatory power) is the total optical activity of the fibre, which amounts to about 5% of the total twist in silica fibre [16,20].

Eq. (1) shows that α allows adjusting the phase bias, and also modifies, through the factor $\cos 2(\alpha - \alpha_c)$, the dynamic

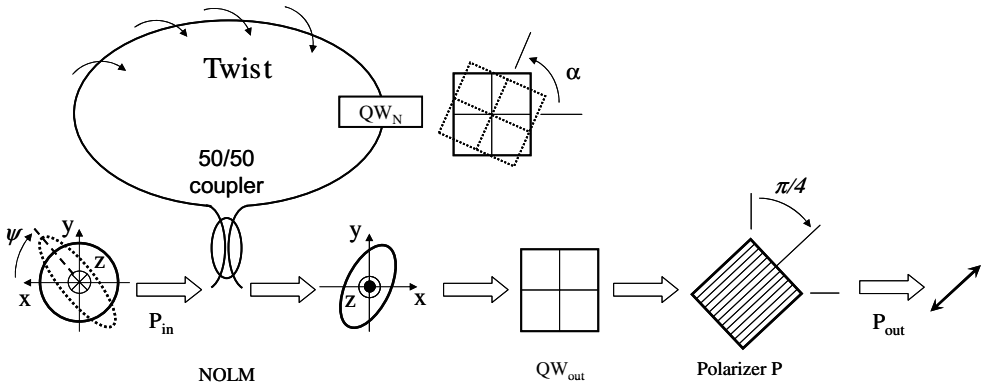

Fig. 1. Scheme considered for the theoretical analysis.

range, defined as the ratio between maximal and minimal transmission values. Hence, starting from $\alpha = \alpha_c$, where the phase bias = 0 and dynamic range is infinite, a modification of α rapidly degrades the dynamic range. In particular, minimal transmission increases rapidly from zero as the curve minimum moves away from $P_{in} = 0$ (Fig. 2a). This has important consequences on the output power characteristic $P_{out} = T_N P_{in}$. Fig. 2b shows that P_{out} monotonously increases at moderate power, showing in particular no local maximum or minimum over the power range under consideration ($P_{in} \ll P_\pi$). This kind of characteristic is of poor interest for signal shaping applications, like amplitude equalisation, where a local maximum of P_{out} is required [11], or extinction ratio enhancement (reduction of the background level on a pulse train, or of ghost pulses, for example), for which a local minimum at $P_{in} > 0$ is preferable [21]. Such extrema only appear in the characteristic of the NPR-based NOLM for input power values above the switching power [13].

The situation is different if one particular polarisation component is selected at the NOLM output. We showed in [22] that, if the circular component of the same sign as the input is selected, the resulting transmission always presents a minimum at $P_{in} = 0$, independently of α, removing all adjustment possibility. In contrast, if the circular component orthogonal to the input polarisation is selected, the transmission (that we denote in this case T_{NP}) is given by

$$T_{NP} = \frac{1}{4} - \frac{1}{4}\cos\left[\pi\frac{P_{in}}{P_\pi} + 4(\alpha - \alpha_c)\right]. \quad (2)$$

In what follows, this configuration will be referred to as NOLM + QW + P. As it can be seen from Eq. (2), α allows to adjust the phase bias, but does not affect the dynamic range, which in this case is infinite (zero minimal transmission). When this bias is slightly positive ($0 < \alpha - \alpha_c \ll \pi/4$), T_{NP} monotonously grows at moderate input power, and so does also the P_{out} characteristic, which is of poor interest for our purposes. In contrast, for slightly negative bias ($-\pi/4 \ll \alpha - \alpha_c < 0$), T_{NP} reaches zero at moderate input power $P_{in} = -4(\alpha - \alpha_c)P_\pi/\pi$ (Fig. 2c). The output power characteristic $P_{out} = T_{NP}P_{in}$ first grows with P_{in}, then reaches a local maximum, and subsequently decreases to reach zero at the point where $T_{NP} = 0$ (Fig. 2d). Because it forces P_{out} to go back to zero at nonzero input power, infinite dynamic range ensures the existence of a maximum and minimum of P_{out} at moderate power (if $\alpha - \alpha_c < 0$). This kind of characteristic is very useful for signal shaping applications. The rotation of the QW_N constitutes a very simple and convenient way to adjust the maximum and minimum

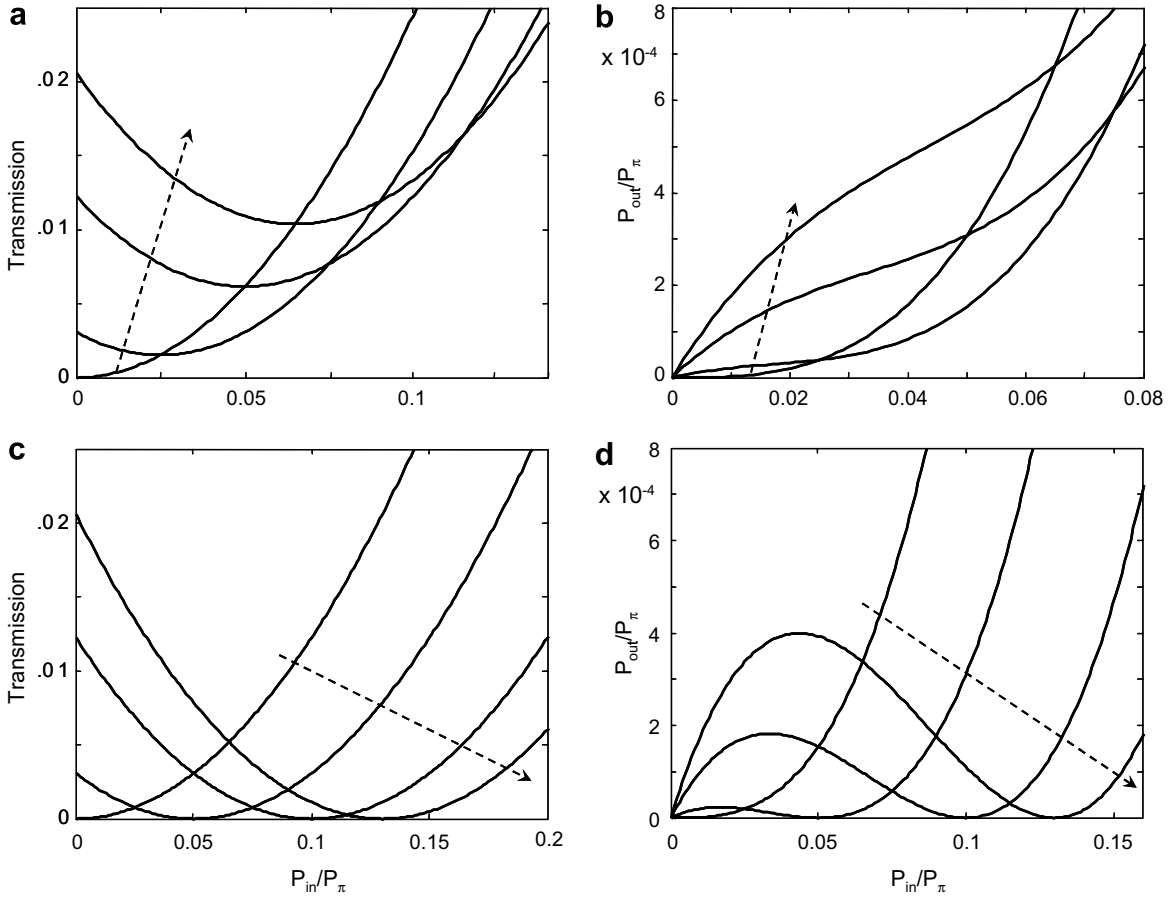

Fig. 2. Nonlinear transmission (a and c) and output power (b and d) characteristics of the NOLM alone (a and b) and of the NOLM + QW + P (c and d) in the case of circular input polarisation. $\alpha - \alpha_c = 0, -.0125\pi, -.025\pi$ and $-.0325\pi$ (in the sense of the arrows).

of the output power characteristic. Another advantage of the configuration is that the output polarisation state is now fixed, and no longer depends on input power.

Infinite contrast is not necessary however to observe a maximum and a minimum in the P_{out} characteristic. In order to study the conditions to be fulfilled for the existence of extrema in P_{out} at moderate power, let us consider a sinusoidal transmission of the general form

$$T \propto \frac{1}{2} - \frac{1}{2}K\cos\left[\pi\frac{P_{in}}{P_{\pi}} - \Delta\phi\right], \tag{3}$$

with $0 \leqslant K \leqslant 1$. As the output power characteristic $P_{out}(P_{in}) = TP_{in}$, it comes that

$$\frac{dP_{out}}{P_{in}} = T + P_{in}\frac{dT}{P_{in}}. \tag{4}$$

The P_{out} characteristic will present a local maximum (minimum) at moderate power if $dP_{out}/dP_{in} = 0$ for some nonzero value of $P_{in} \ll P_{\pi}$. As the power transmission $T \geqslant 0$, a necessary condition is that $dT/dP_{in} \leqslant 0$. T will present a negative slope at moderate power if the phase bias in Eq. (3) is slightly positive, i.e. $0 < \Delta\phi \ll \pi$ (dT/dP_{in} is then negative between $P_{in} = 0$ and the minimum of T at $P_{in} = \Delta\phi P_{\pi}/\pi$). Clearly, the existence or absence of extrema of P_{out} at moderate power will depend on the value of K or, equivalently, on the dynamic range $D = (1 + K)/(1 - K)$, a value ranging between *1* and ∞. To understand this, let us consider two extreme situations. If $D = 1$ ($K = 0$), then T is a constant >0 and $dT/dP_{in} = 0$ for any input power value, so that no value of P_{in} can be found where dP_{out}/dP_{in} vanishes, as shown by Eq. (4). If now $D = \infty(K = 1)$, the situation is similar to the case of Eq. (2): T reaches zero for some nonzero value of P_{in}, so that $P_{out} = TP_{in}$ is forced to decrease to zero after reaching a maximum. In fact, as D (or K) increases from 1 (0), some point eventually appears where T becomes small enough and $|dT/dP_{in}|$ large enough to cancel dP_{out}/dP_{in}, creating a plateau at moderate power. If D (or K) increases further, both a maximum and a minimum appear in the P_{out} curve. There is thus a threshold value of $D < \infty$ above which two extrema appear in the P_{out} characteristic.

The existence of extrema also depends on the value of $\Delta\phi$. The effect of varying this phase bias is to shift the T characteristic along the P_{in} axis. Hence, considering a particular point in the T characteristic, defined by a particular value of the argument $\pi P_{in}/P_{\pi} - \Delta\phi$, a modification of $\Delta\phi$ will modify proportionally P_{in}, i.e. this point will be shifted (together with the whole curve) along the P_{in} axis (to the right if $\Delta\phi$ is increased, otherwise to the left), whereas T and dT/dP_{in} at this point will not be altered. Hence, looking at Eq. (4), a change in $\Delta\phi$ only affects dP_{out}/dP_{in} at each point through the value of P_{in} in the second term of the right-hand side. As a consequence, for a given (finite and >1) value of the dynamic range (thus for fixed T and dT/dP_{in} at each point), and considering the power range where $dT/dP_{in} < 0$, extrema will appear in the P_{out} characteristic if $\Delta\phi$ is large enough, and will be absent if $\Delta\phi$ is too small. For a given D, there is thus also a threshold value of $\Delta\phi$ above which two extrema appear.

We carried out a numerical study about the conditions for the existence of moderate-power extrema of P_{out} in terms of parameters D and $\Delta\phi$, on the basis of Eq. (3). This analysis resulted in the division of the $(D, \Delta\phi)$ plane in two sectors: sector I corresponding to small D and $\Delta\phi$, where P_{out} grows monotonously with power at moderate power ($<P_{\pi}$), and sector II, for large D and $\Delta\phi$, in which the P_{out} characteristic presents a local maximum followed by a minimum at moderate power (Fig. 3a). The line of transition between these two sectors (solid line in Fig. 3a) is the locus of the threshold values of D for a given $\Delta\phi$ (or conversely), and corresponds to the existence of a wide plateau at moderate power in the P_{out} characteristic, where its first

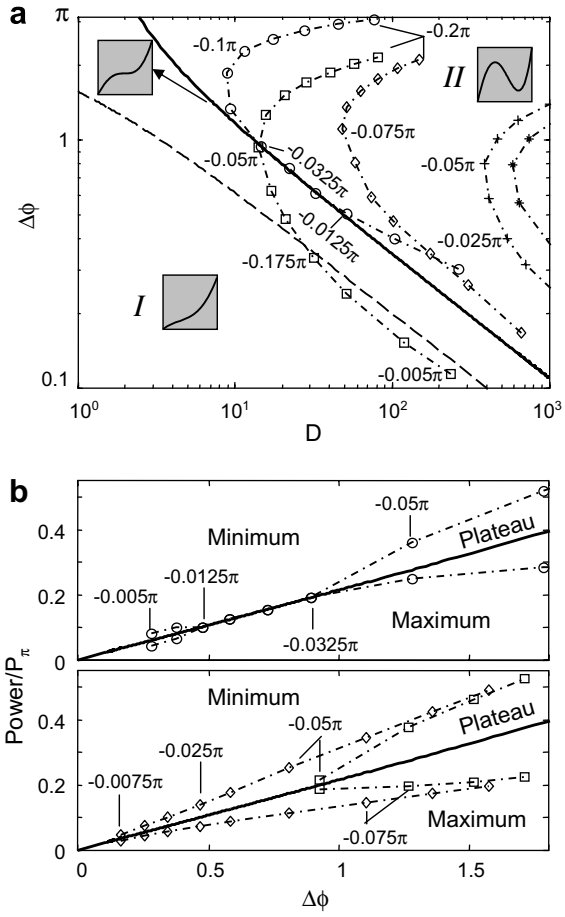

Fig. 3. (a) Division of the (D, $\Delta\phi$) plane in two sectors I (P_{out} grows monotonously) and II (P_{out} presents two extrema). Solid curve marks the transition. The figure includes the characteristic of the NOLM alone (dashed curve), as well as the characteristics of the NOLM + QW + P for $A_s^{cw} = 0.8$ and $\alpha_c + \psi = 0$ (+) and $\pi/8$ (squares), and for $A_s^{cw} = 0.9$ and $\alpha_c + \psi = 0$ (stars), $\pi/8$ (diamonds) and $\pi/4$ (circles). (b) Power, in function of $\Delta\phi$, of the maximum and minimum of the NOLM + QW + P characteristic for $A_s^{cw} = 0.8$ and $\alpha_c + \psi = \pi/8$ (squares, when these two extrema exist), and for $A_s^{cw} = 0.9$ and $\alpha_c + \psi = \pi/8$ (diamonds) and $\pi/4$ (circles). Solid lines give the power of the plateau at transition between sectors I and II. Fig. (b) was split in two for better readability. For each characteristic, $\alpha - \alpha_c$ varies between -0.005π and -0.2π (some values are indicated in the figures).

two derivatives cancel out simultaneously. Solid line in Fig. 3(b) shows the power of the plateau centre, which grows with $\Delta\phi$. Fig. 3a also includes the $(D,\Delta\phi)$ characteristic of the NPR-based NOLM (without QW_{out} and P) under circular input polarisation (dashed line). For $0<|\alpha-\alpha_c|<\pi/4$, comparing Eqs. (1) and (3) yields $\Delta\phi=-2(\alpha-\alpha_c)$, $K=\cos\Delta\phi$ and $D=(1+\cos\Delta\phi)/(1-\cos\Delta\phi)$. It appears clearly from the figure that this characteristic is totally included in sector I, which confirms that no extrema of P_{out} can be expected at moderate power for the NOLM without QW_{out} and P. The curve is interrupted at $\Delta\phi=\pi/2$ (where $D=1$), as beyond this point, $\cos[2(\alpha-\alpha_c)]$ changes sign in Eq. (1), causing a π jump of $\Delta\phi$. The transmission T_N then no longer decreases but instead increases with P_{in} at low power, removing the possibility of finding extrema in this region. For this reason, extrema in the P_{out} characteristic of the power-balanced NOLM can only be found for higher values of input power, which are actually beyond the switching power [13]. In the case of the NOLM + QW + P [Eq. (2)], $D=\infty$, so that the corresponding $(D,\Delta\phi)$ characteristic can not be represented in Fig. 3a. This characteristic is included in sector II, however, and extrema appear at moderate power for arbitrarily small values of $\Delta\phi$.

In experimental conditions, contrast is always finite. In practice, some ellipticity is expected to affect the ideally circular input polarisation, and modify the NOLM + QW + P characteristic given by Eq. (2), in particular reducing its dynamic range. Hence it is important to assess to which extent the local extrema of P_{out} at moderate power can still be found in the case of imperfectly circular, or quasi-circular input polarisation. We derived in [19] an expression for the power transmission of the circular left component of the power-symmetric NOLM, in the general case of any input polarisation, which writes as

$$\begin{aligned}T_{NP}=&\frac{1+A_s^{cw}}{4}\sin^2\left[\frac{A_s^{cw}+A_s^{ccw}}{2}\pi\frac{P_{in}}{P_\pi}+2(\alpha-\alpha_c)\right]\\&+\frac{1-A_s^{cw}}{4}\sin^2\left[\frac{A_s^{cw}-A_s^{ccw}}{2}\pi\frac{P_{in}}{P_\pi}\right]\\&+\frac{1}{2}\sqrt{1-A_s^{cw^2}}\sin\left[\frac{A_s^{cw}+A_s^{ccw}}{2}\pi\frac{P_{in}}{P_\pi}+2(\alpha-\alpha_c)\right]\\&\times\sin\left[\frac{A_s^{cw}-A_s^{ccw}}{2}\pi\frac{P_{in}}{P_\pi}\right]\sin\left[-A_s^{cw}\pi\frac{P_{in}}{P_\pi}+2(\alpha_c+\psi)\right],\end{aligned}\tag{5}$$

where A_s^{cw} and A_s^{ccw} are the first Stokes parameters of the clockwise and counter-clockwise beams, respectively, and ψ is the input polarisation orientation (see Fig. 1). When the NOLM coupler does not affect polarisation, A_s^{cw} also corresponds to the Stokes parameter at the NOLM input. In the counter-clockwise direction, it is turned into $A_s^{ccw}=-\sqrt{1-A_s^{cw^2}}\sin 2(\alpha+\psi)$ through the action of the QW_N (note that, if $|A_s^{cw}|<1$, A_s^{ccw} depends on the angle $\alpha_c+\psi$ between input polarisation and QW_N axes). The right-hand side of Eq. (5) includes three terms. The first one is a sinusoidal function of P_{in}, with a phase bias proportional to $\alpha-\alpha_c$. In the case of circular right input polarisation ($A_s^{cw}=1$), this is the only term left and Eq. (5) reduces to Eq. (2). The second term of Eq. (5) is also a sinusoidal function of P_{in}, but with phase bias = 0. The transmission T_{NP} reduces to this term for circular left input polarisation ($A_s^{cw}=-1$). Finally, the last term is a product of three sinusoidal functions of P_{in}, which vanishes for circular input polarisation.

Although a general analysis of Eq. (5) would be a hard task, some important features at moderate power can be figured out easily in the case of quasi-circular input polarisation (A_s^{cw} close to 1) and $|\alpha-\alpha_c|\ll\pi/4$ (i.e. extrema are expected at moderate power). Fig. 4a shows, for $A_s^{cw}=0.9$, and for some value of α slightly smaller than α_c, the transmission given by Eq. (5), together with its three constitutive terms, at moderate power. The first term corresponds to the transmission obtained in the ideal case of perfectly circular input polarisation, with a sinusoidal dependence that cancels out for some nonzero value of P_{in}. The other two terms will alter this minimum when input polarisation is not perfectly circular. The second term starts growing from zero at $P_{in}=0$, thus reaching some nonzero value where the first term is at minimum. The third term alternatively takes positive and negative values, crossing zero when one of its constitutive factors cancels out. Eq. (5) shows that the argument of the first factor in the third term is identical to the argument of the first term. As a consequence, zero crossing of the third term occurs exactly at the minimum of the first term. Hence, contrary to the second term, the third term does not affect the value of the minimum of the first term, although its slope at the zero crossing slightly shifts this minimum horizontally (compare thick solid and dashed curves). Fig. 4b shows, for several values of α, how evolves the minimum of T_{NP} (solid curves). As α increases, the curve minimum moves to the right and is raised according to the second right-hand term of Eq. (5) (dotted lines). The smaller A_s^{cw}, the larger the slope of the second term, as its amplitude is proportional to $1-A_s^{cw}$, and the minimum of T_{NP} is raised faster with α (compare thick solid, dashed and dashed-dotted curves in Fig. 4b, obtained for the same value of α but different values of A_s^{cw}). Note that the second term of Eq. (5) depends on α, although not explicitly, through A_s^{ccw}. This variation is limited however, as far as $\alpha-\alpha_c$ remains small (see dotted curves in Fig. 4b). Fig. 4c and d shows the P_{out} characteristics for $A_s^{cw}=0.8$ and 0.9, respectively. In the first case, monotonous growth is observed, whereas two extrema appear in the P_{out} characteristics in the second case for $\alpha-\alpha_c<0$ (a similar behaviour is observed for $A_s^{cw}=0.95$). Hence in the case of quasi-circular input polarisation, the existence of extrema of P_{out} at moderate power will be preserved only as far as A_s^{cw} does not deviate too much from 1.

Eq. (5) is not, in general, a simple sinusoidal function of P_{in}, so that the problem of the extrema of P_{out} cannot be tackled, strictly speaking, simply in terms of D and $\Delta\phi$,

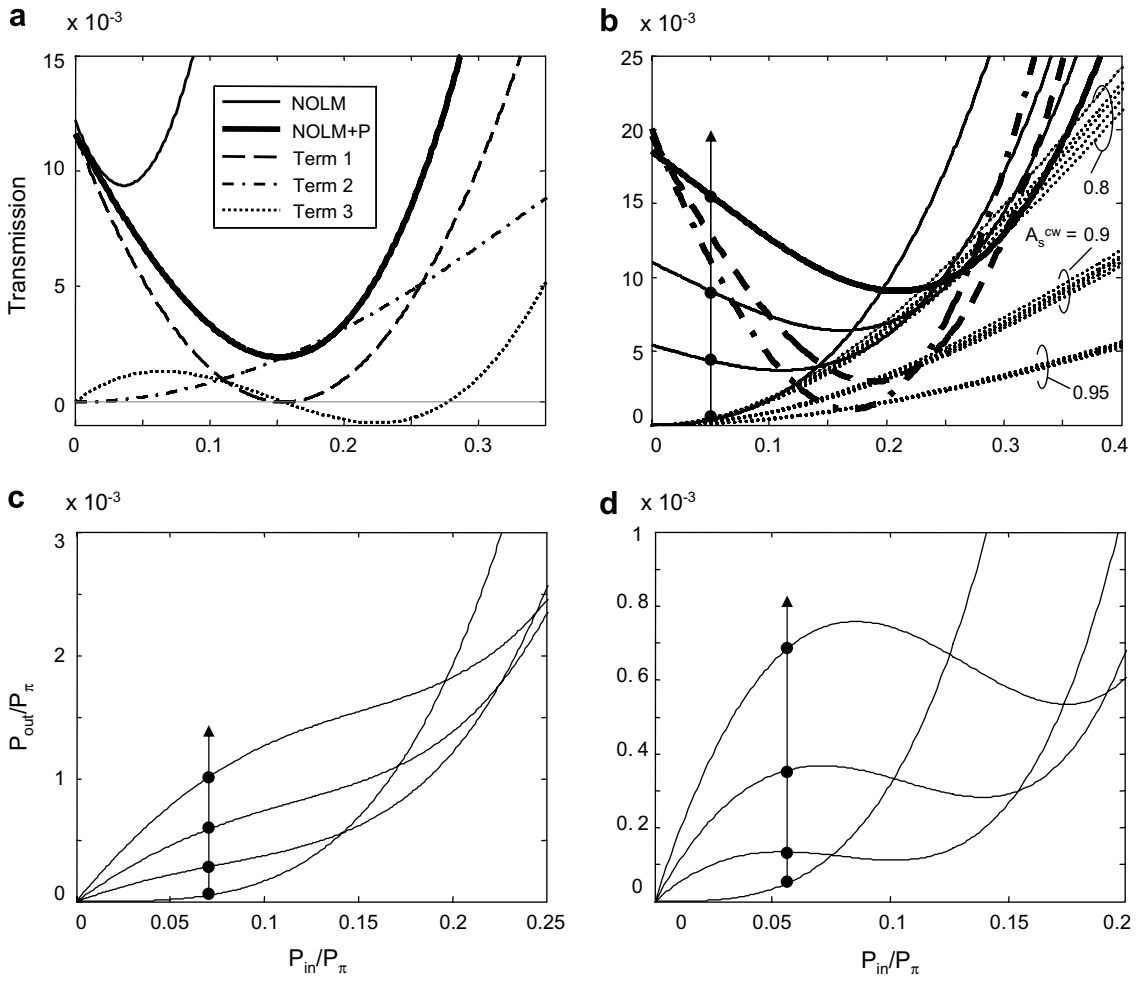

Fig. 4. (a) Transmission characteristics of the NOLM, of the NOLM + QW + P as well as the three terms of Eq. (5), for the parameters $A_s^{cw} = 0.9$, $\alpha - \alpha_c = 0.025\pi$ and $\alpha_c + \psi = 0.125\pi$. (b) NOLM + QW + P transmission for $A_s^{cw} = 0.8$ and $\alpha - \alpha_c = 0$, -0.0175π, -0.025π and -0.0325π (solid lines, in the sense of the arrow), for $A_s^{cw} = 0.9$ and $\alpha - \alpha_c = -0.0325\pi$ (dashed line), and for $A_s^{cw} = 0.95$ and $\alpha - \alpha_c = -0.0325\pi$ (dashed-dotted line). Dotted lines represent the 2nd term of Eq. (5), for each value of A_s^{cw}, which slightly depends on $\alpha - \alpha_c$ (varied between 0 and -0.0325π). NOLM + QW + P output power characteristics are shown for (c) $A_s^{cw} = 0.8$ and (d) $A_s^{cw} = 0.9$, and the same values of $\alpha - \alpha_c$ as previously (in the sense of the arrows). We chose $\alpha_c + \psi = \pi/8$ in all cases.

using Eq. (3). In the case of quasi-circular input polarisation, however, we were able to estimate D and $\Delta\phi$ by fitting the actual transmission [Eq. (5)] with Eq. (3) at moderate power, using the least squares method. We simulated, using Eq. (5), the NOLM + QW + P transmission characteristic for various input polarisation states (i.e. for various values of A_s^{cw} and ψ) and, in each case, we estimated D and $\Delta\phi$ in function of the QW_N angle α.

Results obtained by this procedure are included in Fig. 3a. Each value of input polarisation is associated with a particular characteristic in the $(D, \Delta\phi)$ plane. These results show a strong dependence on the value of A_s^{cw}, as expected, and also on the value of ψ, for a fixed A_s^{cw}. Let us focus our attention on the points for which $|\alpha - \alpha_c| \ll \pi/4$, which correspond to the inferior section of each characteristic in Fig. 3a. In this case, the angle between input polarisation and the $QW_N = \alpha + \psi \approx \alpha_c + \psi$. We first consider the case $A_s^{cw} = 0.9$. When the polarisation axis is roughly parallel with one of the QW_N axes ($\alpha_c + \psi = 0$, stars in Fig. 3a), the characteristic is located in sector II, far from the border with sector I, and the dynamic range is large. The values of D gradually decrease, and the characteristic gets closer to the border as the input polarisation orientation gets away from the QW_N axes (see diamonds for $\alpha_c + \psi = \pi/8$). When input polarisation is oriented at 45° with respect to the QW_N axes ($\alpha_c + \psi = \pi/4$, circles), several points of the characteristic appear on the border, meaning that for these values of α a plateau appears in the P_{out} curve (see also Fig. 3b, circles). A similar evolution is observed for $A_s^{cw} = 0.8$, but in this case, the inferior section of the characteristic appears in sector I when the polarisation orientation deviates too much from the QW_N axes (see Fig. 3a for $\alpha_c + \psi = \pi/8$, squares).

Without carrying out a detailed analysis of Eq. (5), this dependence on ψ of the $(D, \Delta\phi)$ characteristic can be understood simply by considering the following. In the ideal case of circular input polarisation ($A_s^{cw} = 1$), the polarisation of the counter-clockwise beam is made linear by the QW_N ($A_s^{ccw} = 1$). In the case of quasi-circular input polarisation,

the polarisation of the counter-clockwise beam depends on the orientation $\alpha+\psi$ of the input polarisation with respect to the QW_N. If $\alpha+\psi=0$, $A_s^{ccw}=0$ and the counter-clockwise beam is still linear, so that the modifications with respect to the ideal case (were D is infinite) are minimal in this case. In contrast, if $\alpha+\psi=\pi/4$, A_s^{ccw} is maximum for a given A_s^{cw} (for example, $A_s^{cw}=0.9$ yields $A_s^{ccw}=-\sqrt{1-A_s^{cw^2}}=-0.43$), so that major changes are observed, in particular D is substantially reduced, and the existence of extrema of P_{out} at moderate power can be jeopardised. For $A_s^{cw}=0.9$ or higher, the curves do not cross the border into sector I, showing that these values are compatible with signal reshaping applications. In contrast, this crossing happens for lower values of A_s^{cw}, for some orientations of the input polarisation. Considering, for example, the case $A_s^{cw}=0.8$ and $\alpha_c+\psi=\pi/8$ (squares in Fig. 3a), points corresponding to the small values of α appear in zone I. Extrema will only appear in the P_{out} characteristic if $|\alpha-\alpha_c|$ is increased beyond 0.05 π (corresponding to $\Delta\phi\approx 1$ rad), yielding relatively high values for the powers at which these extrema occur (see Fig. 3b, squares). It has to be noted that, except in the particular case of perfectly circular input polarisation, where Eq. (2) applies, so that $\Delta\phi=-4(\alpha-\alpha_c)$, the relation between $\alpha-\alpha_c$ and $\Delta\phi$ is not linear in general, even if $\Delta\phi$ [obtained through fitting Eq. (3) with Eq. (5)] is still a growing function of $-(\alpha-\alpha_c)$. Finally, it has to be observed that, for all the $(D,\Delta\phi)$ characteristics, as $|\alpha-\alpha_c|$ is increased (as $\Delta\phi$ is increased), the dynamic range first decreases, reaches a minimum and then increases again. This is related to the sinusoidal nature of the second term in Eq. (5) (which determines the value of the minimum of T_{NP}): it increases at low power, then reaches a maximum and decreases as P_{in} approaches P_π. The characteristics beyond the minimum of D have limited interest however for our purposes, as for these points the extrema appear at relatively large power.

3. Experimental results and discussion

We tested the efficiency of the proposed scheme for pulse shaping applications using the experimental setup shown in Fig. 5. The NOLM included a ~51/49 coupler, 500 m of highly twisted (7 turns/m) standard SMF-28 fibre, and a QW (QW_N) made by wrapping one end of the fibre on a disk of appropriate diameter. Although the coupler is slightly asymmetric, the resulting power imbalance does not produce significant SPM contribution to the switching mechanism [17]. The switching power was $P_\pi\approx 30$ W. As the input signal, we used the 1549-nm emission of a DFB laser diode, which was amplified by a two-stage Erbium-doped fibre amplifier (EDFA). In a first step, the laser was biased at ~20 mA (above threshold) to operate in continuous wave. The input signal polarisation to the NOLM was made roughly circular using a polarizer P1 followed by a QW (QW1) at the NOLM input. To ensure that circularly polarized light was effectively injected into the NOLM, light polarisation of the collimated beam was measured at the coupler outputs prior to splicing, using free-space QW, polarizer and power meter. The polarizer P1 orientation at the NOLM input was then adjusted to maximise the ratio P_{max}/P_{min} between the powers in each circular polarisation component. A value of ~200 was obtained ($A_s^{cw}\approx 0.99$). Transmission through polarizer P1 was then maximised using a polarisation controller, and the coupler output ports were finally spliced to the fibre ends. By measuring power at the NOLM output, we observed, as expected, that low-power transmission varies periodically with the QW_N angle α [18]. The QW_N angle α was set away from minimal low-power transmission. A QW (QW2) and a polarizer (P2) were then inserted at the NOLM output to select the circular component orthogonal to the input polarisation. This was ensured by orientating the axes of the QW2 and P2 at 45° with respect to each other, in the direction that maximised the output power through the polarizer at low power.

To characterise the nonlinear transmission of the setup, the DFB laser was biased at ~5 mA, slightly below threshold, and directly modulated with ns squared current pulses to generate ns optical pulses at a rate of ~100 Hz. Both input and output signals were detected using 1-GHz InGaAs photodetectors and were monitored using a two-channel, 500-MHz bandwidth oscilloscope (a 99/1 coupler was used to extract a small fraction of input power for monitoring). The QW_N angle was slightly detuned from minimal low-power transmission. By adjusting the amplitude of the current pulses, the power of the optical pulses amplified by the 2-stage EDFA was varied between ~0 and 6 W at

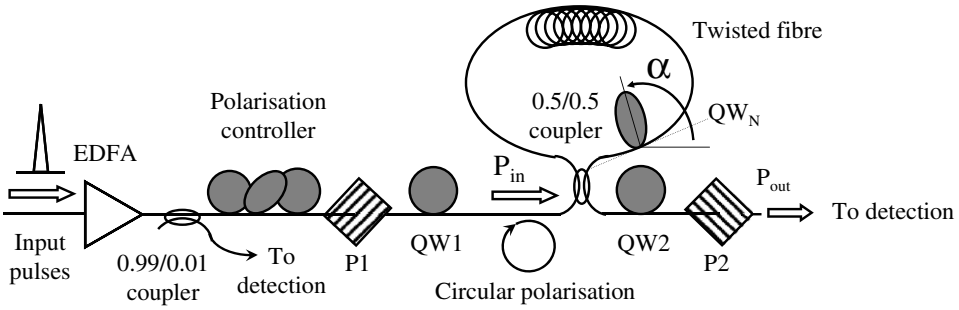

Fig. 5. Experimental setup.

the NOLM input. Power was thus not raised beyond ~20% of switching power for transmission measurements. For one sign of detuning, transmission appeared to grow monotonously with power, and for the other sign, transmission presented a minimum at moderate power. Characteristics obtained in this case for two slightly different adjustments of the QW_N angle (at about 2° and 5° from minimal low-power transmission) are presented in Fig. 6. The P_{out} characteristic presented a maximum followed by a minimum in one case, and a wide plateau in the other case. Such features are attractive for signal shaping applications, in spite of the low transmission values. Characteristics for zero detuning are also shown for comparison.

To demonstrate the signal shaping capabilities of the setup, we again used as a source the directly modulated DFB laser modulated by squared current pulses and amplified by the two-stage EDFA. Pulse duration was set to 30 ns. The generated optical waveforms were not perfectly squared, but instead presented a short ~2-ns initial pulse followed by a long plateau, with a power ratio of about 2 to 1 (Fig. 7a). Moreover, the plateau itself presented a slightly negative slope and substantial intensity fluctuations. In practice, one may want well-shaped squared pulses instead of these irregular waveforms. Using the proposed NOLM-based setup, we made attempts to equalise the waveform so as to get as close as possible to the ideal squared pulse shape. Using the QW_N adjustment of the diamond curve in Fig. 6b, we adjusted the current pulses so as to set the plateau power around the peak of the P_{out} characteristic (~0.7 W). The resulting waveform is shown in Fig. 7b, dashed. The slope of the plateau was cancelled, and its fluctuations were substantially reduced. However, as the power of the initial pulse was ~1.5 W at the NOLM input, nearly corresponding to the minimum of the P_{out} characteristic, its power at the output was reduced below the plateau level. A more efficient power equalisation was obtained for the QW_N adjustment corresponding to the squares curve in Fig. 6b. The result is shown in Fig. 7b, solid curve, when the plateau power at the input is set to ~1.5 W (and pulse power to ~3 W). Thanks to the wide flat region of the P_{out} characteristic, we obtained in this case a rather uniform, nearly squared pulse. The strongest residual amplitude fluctuation observed in the output waveform is caused by the deep tough appearing just after the pulse in the initial waveform, as its power (~1.2 W) is slightly outside the flat region of the P_{out} characteristic.

Another important pulse shaping application consists in enhancing the extinction ratio. A typical example is the reduction of background noise or ghost pulses in data trains. To illustrate the capabilities of our setup in this frame, we attempted to reduce the plateau level of the waveform of Fig. 7a as much as possible with respect to the initial pulse. The best results were obtained using the diamonds curve in Fig. 6b, whose dynamic range is higher. Beginning with the input plateau power set at ~0.7 W and pulse power at ~1.5 W, we started to increase power. As the plateau power approaches the minimum of the P_{out} characteristic, it gets flattened, but the initial pulse starts to grow with respect to the plateau, as its input power goes beyond the minimum of the P_{out} characteristic (see dashed curve in Fig. 7c, note also the substantial shortening of the initial pulse in this case, whose duration shown here is at the limit of the scope resolution). If power is further increased, the pulse continues to grow with respect to the plateau. The maximal contrast is reached for a plateau power ~2 W (slightly beyond minimal P_{out}) and a peak power ~4 W (solid curve in Fig. 7c). The figure shows that the plateau almost completely disappears in this case (oscillations following the pulse are related to the impulse response of the detection setup). If power is increased beyond this point, a very uneven plateau reappears (dotted curve in Fig. 7c).

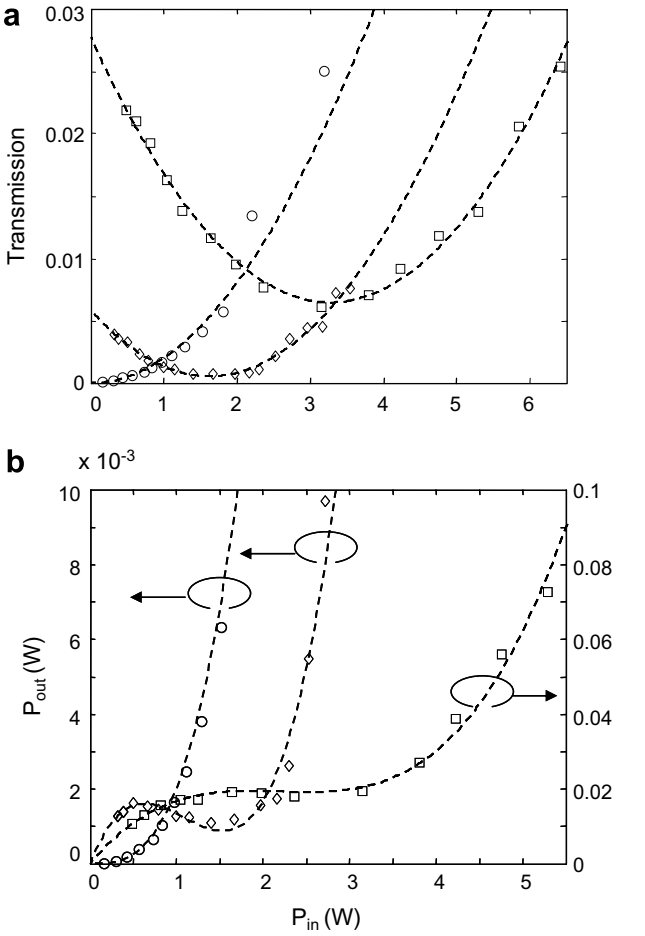

Fig. 6. (a) Experimental NOLM + QW + P transmission (a) and output power (b) characteristics for $|\alpha - \alpha_c| = 0$ (circles), ~2° (diamonds) and ~5° (squares). Two different scales were used for the ordinates of Fig. (b) for better readability.

We also used the NOLM-based setup to shape ultrashort pulses from the waveforms generated by the DFB laser. In this case, the duration of current pulses was reduced to its minimal value of 2 ns, so that the plateau was removed from the optical waveform, which was reduced to the short 2-ns pulse. Monitoring this pulse using a 10-GHz photodetector and a 20-GHz sampling scope

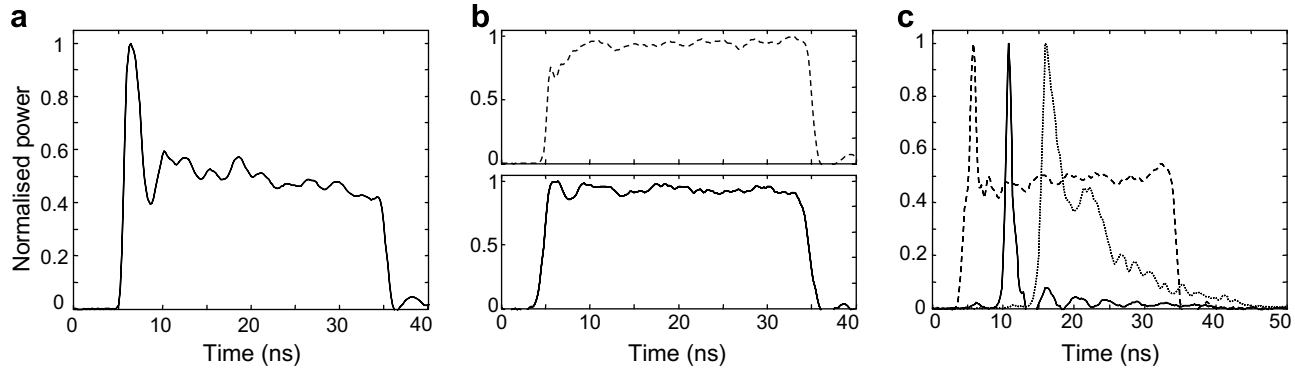

Fig. 7. (a) Waveform used for pulse shaping demonstration. (b) Results of equalisation for $|\alpha - \alpha_c| = 2°$ and peak power = 1.5 W (dashed), and for $\alpha - \alpha_c = 5°$ and peak power = 3 W (solid). (c) Output waveforms for $\alpha - \alpha_c = 2°$ and peak power = 2.3 W (dashed), 4 W (solid) and 6 W (dotted). All waveforms are normalised with respect to peak power.

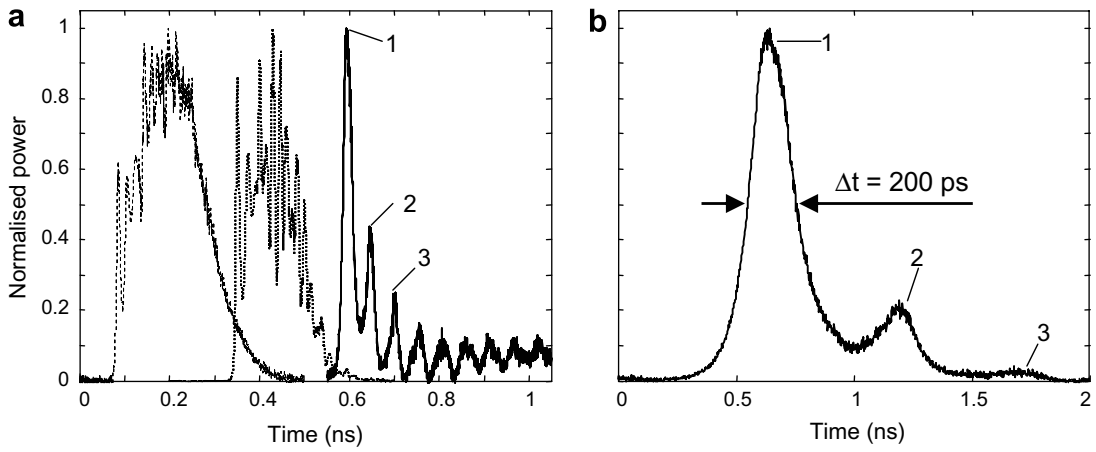

Fig. 8. (a) Waveforms obtained from the DFB laser with 2-ns drive current pulses of 35 mA (dashed), 25 mA (dotted) and 7 mA (solid). (b) Waveform at the output of the NOLM + QW + P for 7-mA current pulses. All waveforms are normalised with respect to peak power.

revealed an ultrafast amplitude modulation pattern with a period ranging between ~120 and ~500 ps, depending on the level of current pulses (Fig. 8a). This modulation with power-dependent frequency is the signature of the relaxation oscillations of the laser diode, which are triggered by the rising edge of the current pulses. The optical spectrum of the 2-ns pulses also revealed the presence of relaxation oscillations, through the two side lobes appearing at ~5 GHz from the main peak (for ~20-mA drive current). When the current pulses barely exceed threshold (~5 mA), the initial spike is substantially higher than subsequent oscillations (Fig. 8a, solid). We used the NOLM + QW + P setup to improve the extinction between the initial spike and these oscillations. After amplification through the 2-stage EDFA, the waveform was launched into the NOLM. The signal emerging from the output polarizer was then detected and monitored on the sampling scope. The QW_N angle was adjusted over a range of a few degrees until the highest extinction was obtained. The best result is shown in Fig. 8b. The resulting pulse had a duration of ~200 ps. A residual second peak of oscillation was still present up to ~20% of the initial peak power, but the third one was very low (~2.5%), and subsequent peaks of the input waveform were not detected at the output. This demonstrates a simple technique to generate ultrashort optical pulses from a directly modulated semiconductor laser, in which the electrical bandwidth of modulation is not higher than several hundreds of MHz. Pulse duration is mainly determined by the frequency of relaxation oscillations, which typically ranges as various GHz or higher.

4. Conclusion

In conclusion, we showed that using a high-twist NPR-based NOLM in which the circular output polarisation component orthogonal to the input is selected, optical pulse shaping is possible for moderate input power levels, at the price of low values of transmission. Thanks to the outstanding properties of highly twisted fibre, the phase bias of the transmission can be precisely controlled simply through the rotation of a quarter-wave retarder. This precise adjustment capability is a key condition to maintain extrema at moderate power in the output power character-

istic. We studied numerically the tolerance of these extrema to a modification of the input polarisation from the ideally circular case. Results showed that reasonably small polarisation excursions do not jeopardize the signal shaping capabilities of the setup. The setup was implemented experimentally and employed to shape a nanosecond optical waveform, which was composed of a pulse and an uneven pedestal in a ratio of about 2:1. The proposed setup made it possible to equalise the uneven waveform, which was levelled off into a nearly squared pulse with a residual power fluctuation of ~10%. In another experiment, we improved the extinction ratio between the pulse and the plateau, resulting in a value of ~50. Although experiments were performed using ns pulses, the procedure is still valid for shaping ps pulses, if NOLM dispersion is properly managed. We also demonstrated experimentally the capabilities of this setup to tailor sub-ns pulses out of high-frequency relaxation oscillations of a semiconductor laser. In all cases, input peak power has not to be raised beyond ~1/8 of the switching power for optimal signal shaping operation. By using this principle, and taking advantage of the recent developments in highly nonlinear photonic crystal fibres, a compact NOLM design could emerge for shaping signals whose peak powers do not exceed a few 100 mW.

Acknowledgement

O. Pottiez was supported by CONCYTEG Grant 07-04-K662-043 and by CONACyT grant 53990.

References

[1] N.J. Doran, D. Wood, Opt. Lett. 13 (1988) 56.
[2] A. Bogoni, L. Poti, R. Proietti, G. Meloni, F. Ponzini, P. Ghelfi, Electron. Lett. 41 (2005) 435.
[3] S. Boscolo, S.K. Turitsyn, IEEE Photon. Technol. Lett. 16 (2004) 1912.
[4] S. Oda, A. Maruta, IEEE Photon. Technol. Lett. 18 (2006) 703.
[5] T. Sakamoto, K. Kikuchi, IEEE Photon. Technol. Lett. 17 (2005) 1058.
[6] K. Cvecek, G. Onishchukov, K. Sponsel, A.G. Striegler, B. Schmauss, G. Leuchs, IEEE Photon. Technol. Lett. 18 (2006) 1801.
[7] J.H. Lee, T. Tanemura, Y. Takushima, K. Kikuchi, IEEE Photon. Technol. Lett. 17 (2005) 840.
[8] A. Bogoni, P. Ghelfi, M. Scaffardi, L. Potì, IEEE J. Sel. Topics Quantum Electron. 10 (2004) 192.
[9] R. Adams, M. Rochette, T.T. Ng, B.J. Eggleton, IEEE Photon. Technol. Lett. 18 (2006) 469.
[10] Y.T. Chieng, G.J. Cowle, IEEE Photon. Technol. Lett. 7 (1995) 485.
[11] M. Attygalle, A. Nirmalathas, H.F. Liu, IEEE Photon. Technol. Lett. 14 (2002) 543.
[12] M. Meissner, R. Rösch, B. Schmauss, G. Leuchs, IEEE Photon. Technol. Lett. 15 (2003) 1297.
[13] O. Pottiez, E.A. Kuzin, B. Ibarra-Escamilla, F. Gutiérrez-Zainos, U. Ruiz-Corona, J.T. Camas-Anzueto, IEEE Photon. Technol. Lett. 17 (2005) 154.
[14] T. Tanemura, K. Kikuchi, J. Lightwave Technol. 24 (2006) 4108.
[15] E.A. Kuzin, B. Ibarra-Escamilla, R. Rojas-Laguna, J. Sanchez-Modragon, Opt. Commun. 149 (1998) 73.
[16] E.A. Kuzin, N. Korneev, J.W. Haus, B. Ibarra-Escamilla, J. Opt. Soc. Am. B 18 (2001) 919.
[17] O. Pottiez, E.A. Kuzin, B. Ibarra-Escamilla, J.T. Camas-Anzueto, F. Gutiérrez-Zainos, Electron. Lett. 40 (2004) 892.
[18] O. Pottiez, E.A. Kuzin, B. Ibarra-Escamilla, J.T. Camas-Anzueto, F. Gutiérrez-Zainos, Opt. Exp. 12 (2004) 3878.
[19] O. Pottiez, E.A. Kuzin, B. Ibarra-Escamilla, F. Mendez-Martinez, Opt. Commun. 254 (2005) 152.
[20] R. Ulrich, A. Simon, Appl. Opt. 18 (1979) 2241.
[21] A. Striegler, B. Schmauss, IEEE Photon. Technol. Lett. 18 (2006) 1058.
[22] O. Pottiez, E.A. Kuzin, B. Ibarra-Escamilla, F. Méndez-Martínez, Opt. Commun. 229 (2004) 147.